FATIGUE CRACK GROWTH IN AlCu4Mg1 UNDER NON-PROPORTIONAL BENDING WITH TORSION LOADING

D. ROZUMEK, Z. MARCINIAK

Opole University of Technology, Poland

The paper presents the experimental results of fatigue crack growth on AlCu4Mg1 aluminium alloy under proportional and non-proportional bending with torsion obtained at Opole University of Technology. Specimens with square sections and stress concentrations in the form of external one-sided sharp notches were used. The tests were performed in the high cycle fatigue regime for the stress ratio $R = -1$ and phase shift between bending and torsion loading equal to $\phi = 0$; 45° and 90°. Three paths of loading were used: line, ellipse and circle. The fatigue crack growth was cyclically measured with use of the optical microscope (magnification of 25 times), strain gauges and computer allow to register signals of loading. In the tested specimens, it was possible to observe growth of cracks conforming with mixed mode I + III. The crack growths were non-uniform at both sides of the specimen surface, however the difference between crack lengths was rather small. In the biaxial tests, influence of bending was six times greater because of the notches in the bending plane. The test results were described by the stress intensity factor range, ΔK.

Key words: *fatigue crack growth rate, out-of-phase loading, mixed mode I + III, notch.*

Development of some modern mechanical structures must include problems connected with strength and fatigue life. Fatigue crack growth occurring in many structures and devices is especially important. Crack growth under simple loading (for example, tension, bending or torsion) is often presented in literature, while problems connected with multiaxial loading are discussed rather rarely [1, 2]. The solved problems of crack growth under complex stress states usually concern proportional loadings [3–5]. Tests of fatigue crack growth under non-proportional loadings are rarely performed because it is difficult to describe experimental results. Some data concerning such tests are published in [6]. The authors tested the growth of short fatigue cracks under mixed mode I+II. The obtained results were described with the J-integral and new relations for correlation of the test results using the J-integral and the influence of surface roughness were proposed. In [7], the authors presented fatigue crack paths for two steels subjected to non-proportional tension-compression with torsion. The various theoretical models were applied for description of the test results.

The aim of this paper is to investigate fatigue crack growth rate in plane specimens under proportional and non-proportional bending with torsion. The tested specimens were made of AlCu4Mg1 aluminium alloy.

Test material and experimental procedures. Specimens with square sections were tested. Beams of such a shape were used: torsion bars in cars (Renault), trucks and tanks (attachment of springs), and intermediate beams for gas and oil wells. AlCu4Mg1 aluminium alloy included in the standard EN AW-2024 and PN-92/H-93667 was subjected to tests. The tested material belongs to a group of medium-alloy duralumins. Specimens with rectangular cross-sections and dimensions: length $l = 90$ mm, height $w = 9.5$ mm and thickness $g = 8$ mm were tested (see Fig. 1). Each specimen had an external unilateral notch with depth 1.5 mm and radius $\rho = 0.2$ mm. The notches in the specimens

Corresponding author: D. ROZUMEK, e-mail: d.rozumek@po.opole.pl

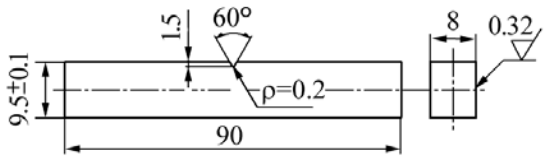

Fig. 1. Specimen for fatigue crack growth tests, dimensions in mm.

were cut with a milling cutter and their surfaces were polished after grinding. Chemical composition and some mechanical properties of the tested aluminium alloy are given in Tables 1 and 2. Strain-based fatigue curves are shown in Fig. 2, where elastic and plastic components are given too. As usual, such curves are described by a linear law in a log-log diagram, as suggested by the Manson–Coffin model. In the same figures, some stabilised hystheresis loops are displayed too. Coefficients of the Ramberg–Osgood equation describing the cyclic strain curve under tension-compression conditions with $R_\varepsilon = -1$ for AlCu4Mg1 aluminium alloy (hardening alloy) are the following [8]: the cyclic strength coefficient $K' = 563$ MPa, the cyclic strain hardening exponent $n' = 0.033$.

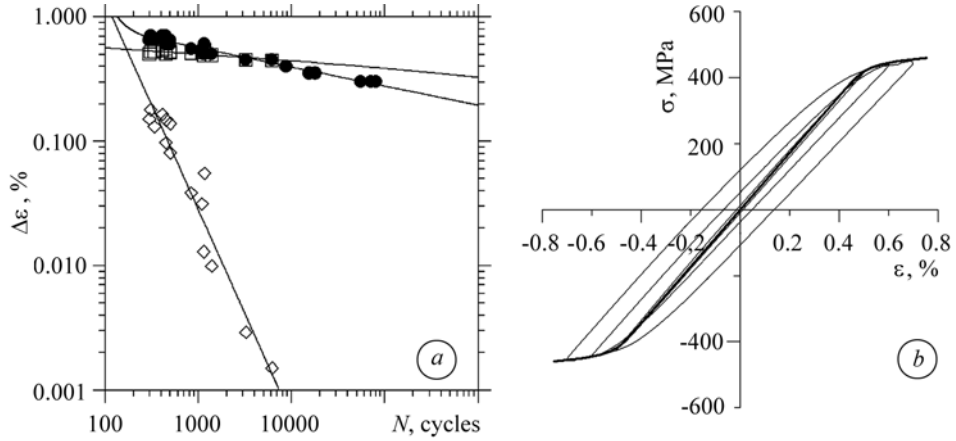

Fig. 2. Fatigue curves under strain control (*a*) and some stabilized hysteresis loops (*b*) of AlCu4Mg1 aluminium alloy. ●, □, ◇ – total, elastic and plastic strains.

Table 1. Chemical composition (wt.%) of AlCu4Mg1 aluminium alloy

Cu	Mn	Zn	Mg	Fe	Cr	Si	Ti	Al
4.15	0.65	0.50	0.69	0.70	0.10	0.45	0.20	Balance

Table 2. Monotonic mechanical properties of $AlCu_4Mg_1$ aluminium alloy

Yield stress	σ_y, MPa	382
Ultimate stress	σ_u, MPa	480
Young's modulus	E, GPa	72
Poisson's ratio	ν	0.32

The static and cyclic properties for AlCu4Mg1 aluminium alloy were obtained from the tests done in the laboratory of the Department of Mechanics and Machine Design of the Opole University of Technology, Poland. The theoretical stress concentration factor in the specimen under bending $K_t = 3.76$, was estimated with use of the model [9].

Fatigue tests were performed in the high-cycle fatigue regime (HCF) at the stress ratio $R = -1$. The tests were carried out on fatigue test stand MZGS-100Ph [10] under controlled loading where the ratio of torsion moment to bending moment was $M_T(t)/M_B(t) = 1$ and loading frequency was 26.5 Hz. The total moment $\bar{M}(t) = \bar{M}_T(t) + \bar{M}_B(t)$ was generated by forces on the arms 0.2 m in length. Shear stress on a fatigue test stand MZGS-100Ph caused by bending takes very small values, below 2% of the maximum normal stress.

Unilaterally restrained specimens were subjected to cyclic bending with torsion

with the constant amplitude of moment $M_a = M_{aB} = M_{aT} = 5.70$ N·m, which corresponded to the nominal amplitude of normal stresses $\sigma_a = 66.80$ MPa and the nominal amplitude of shear stresses $\tau_a = 53.52$ MPa before crack initiation. Crack growth was observed on the specimen surface with the optical method. The fatigue crack increments were measured with a micrometer located in the portable microscope with magnification of 25 times and accuracy 0.01 mm. At the same time, a number of loading cycles N was written down. Under bending with torsion, dimension a of the crack growth was defined as increments of length and angle α_1 between mode I and mode III of the crack measured on the specimen side surface.

Stress distribution. If the specimen is both bended by moment M_B and twisted by moment M_T, in a given rectangular square section normal stresses are formed under the influence of bending and the shear stresses result from torsion. The normal stresses change from zero in the neutral zone z to the maximum value $\sigma_a = \dfrac{6M_B}{gw^2}$ in the extreme fibres (σ_{max}) (Fig. 3). Shear stresses occur, changing from zero in the specimen axis to the maximum value $\tau_a = \dfrac{M_T}{k_1 w g^2}$ ($k_1 = 0.208$ – ratio of the height to the thickness of specimen) at the most distant points from the y axis of the specimen (τ_{max}) (Fig. 3).

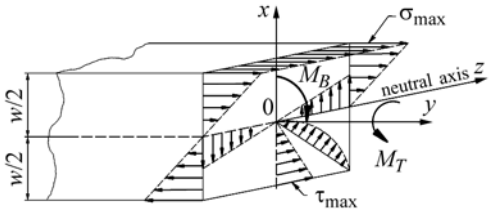

Fig. 3. Normal and shear stress distribution under bending with torsion.

De Saint-Venant worked on the problem of stress distribution under torsion. He found that stresses were equal to zero inside and in the corners of the bar, and they were the biggest in the centers of square sides (longer sides of the rectangle). In the specimen under torsion, cross-sections do not remain plane but are subjected to deformation or the so-called deplanation. If torsion is unfree (as in the presented case), the shear and normal stresses, induced by torsion occur. In the given case, the normal stresses were about six times greater than shear stresses (due to the occurence of the notch in the plane of their action). Under simultaneous action of the two moments, M_B and M_T, the most dangerous stress state is formed in the planes most distant from both the neutral z and y axes of the specimen (Fig. 3 – σ_{max}). The stress area distribution near the crack tip for modes I, II and III is shown in [5]. The stress intensity factors can be expressed as: for mode I $K_I = Y_1 \sigma_a \sqrt{\pi a}$, and for mode III $K_{III} = Y_3 \tau_a \sqrt{\pi a}$.

The analytical models. ***Concept of the ΔK-criterion.*** The obtained test results allow to analyse fatigue crack growth in AlCu4Mg1 aluminium alloy under proportional and non-proportional bending with torsion loading. The test results were shown as graphs of the crack length a versus the number of cycles N and fatigue crack growth rate da/dN versus the ΔK.

The experimental results of fatigue crack growth rate as a function of the stress intensity factor range were described with the Paris equation [11]

$$\frac{da}{dN} = C(\Delta K)^m, \tag{1}$$

where $\Delta K = K_{max} - K_{min}$ and $\Delta K = \Delta K_{eq}$, ΔK_I, ΔK_{III}, respectively; K_{max}, K_{min} – maximum and minimum stress intensity factor respectively.

The range of the equivalent stress intensity factor ΔK_{eq} under mixed mode I+III reduced to mode I can be written as

$$\Delta K_{eq} = \frac{\Delta K_{\mathrm{I}}}{\sqrt{2}} \sqrt{1 + 0.75\left(\frac{2\Delta K_{\mathrm{III}}}{\Delta K_{\mathrm{I}}}\right)^2 + \sqrt{1 + 1.5\left(\frac{2\Delta K_{\mathrm{III}}}{\Delta K_{\mathrm{I}}}\right)^2 \cos 2\phi + 0.5625\left(\frac{2\Delta K_{\mathrm{III}}}{\Delta K_{\mathrm{I}}}\right)^4}} \quad . \quad (2)$$

The equation (2) was obtained from the modified Huber–Mises equation [12]. It allows to calculate the stress intensity factor range under proportional and non-proportional loadings. The results of Eq. (2) were compared with the results obtained from the Huber–Mises equation $\Delta K_{eq} = \sqrt{\Delta K_{\mathrm{I}}^2 + 3\Delta K_{\mathrm{III}}^2}$ for proportional loading. The results of calculations obtained from both equations were similar.

The ranges of stress intensity factors ΔK_{I} for mode I and ΔK_{III} for mode III are the following:

$$\Delta K_{\mathrm{I}} = Y_1 \Delta\sigma \cos^2 \alpha \sqrt{\pi(a_0 + a)}\,, \quad (3)$$

$$\Delta K_{\mathrm{III}} = Y_3 \Delta\sigma \sin\alpha \cos\alpha \sqrt{\pi(a_0 + a)}\,. \quad (4)$$

where $\Delta\sigma$ is the stress range; a_0 is notch length.

For modes I and III [13, 14] the correction coefficients take the forms

$$Y_1 = 5 / \sqrt{20 - 13((a_0 + a)/w) - 7((a_0 + a)/w)^2}\,, \quad (5)$$

$$Y_3 = \sqrt{(2w/(a_0 + a))\tan(\pi(a_0 + a)/(2w))}\,. \quad (6)$$

Test results and their analysis. The fatigue crack growth tests under proportional and non-proportional bending with torsion in AlCu4Mg1 aluminium alloy were performed under controlled loading. During tests, a number of cycles to the crack initiation N_i (i.e. to the moment of occurrence of a visible crack) was determined, and the fatigue crack lengths were measured. The tests were performed under combination of bending and torsion in-phase and 45° out-of-phase and 90° out-of-phase (see Fig. 4). Fig. 4 shows exemplary histories of proportional and non-proportional loadings.

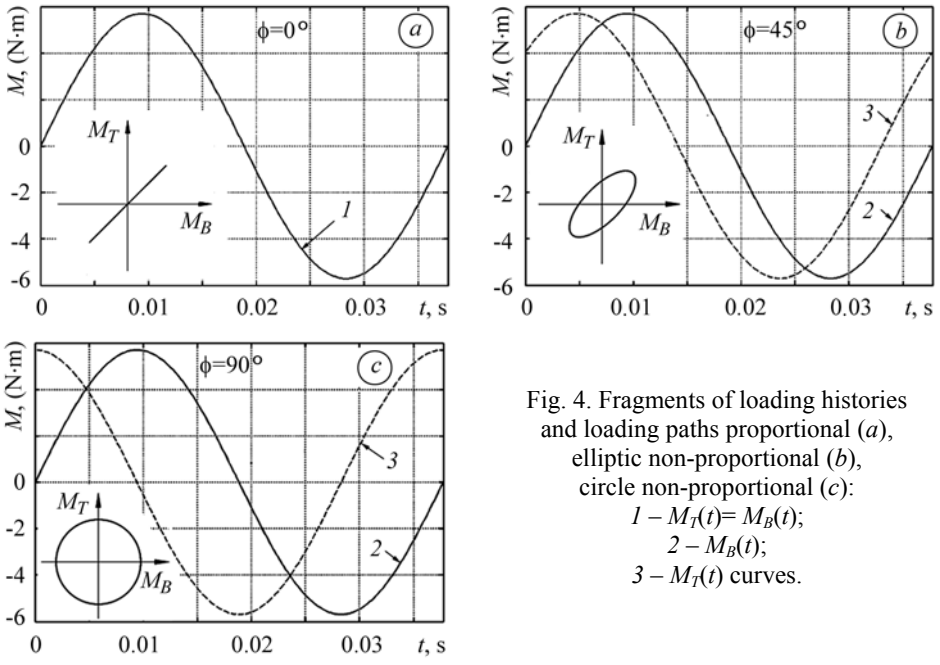

Fig. 4. Fragments of loading histories and loading paths proportional (*a*), elliptic non-proportional (*b*), circle non-proportional (*c*):
1 – $M_T(t) = M_B(t)$;
2 – $M_B(t)$;
3 – $M_T(t)$ curves.

The test results were shown as graphs of the crack length *a* versus the number of cycles *N* and fatigue crack growth rate *da*/*dN* versus the stress intensity factor range ΔK. From the graphs in Fig. 5 it appears that as the phase shift ϕ between bending and

torsion loading increases from 0 to 90°, the fatigue life of the specimens decreases (symbols are used, □ – ϕ = 0, △ – ϕ = 45°, ◇ – ϕ = 90°).

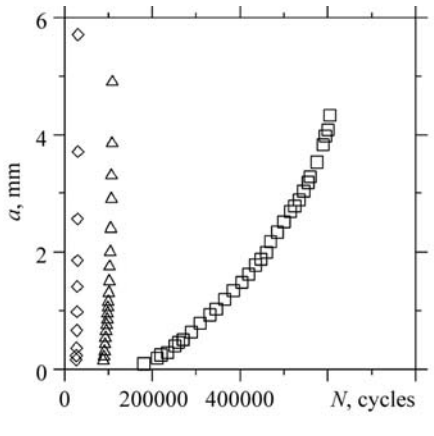

Fig. 5.

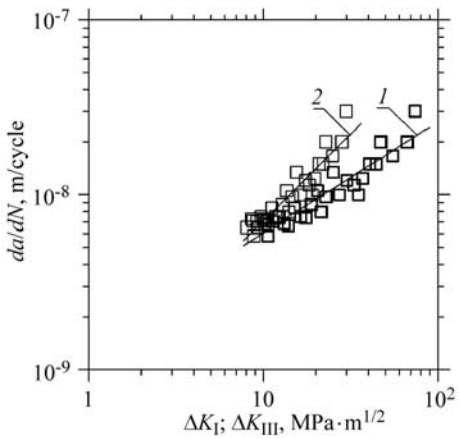

Fig. 6.

Fig. 5. Dependences of fatigue crack length, a, versus number of cycles, N, under non-proportional bending with torsion. M_a = 5.7 N · m; ◇ – ϕ = 90°; △ – 45°; □ – ϕ = 0°.

Fig. 6. Comparison of the experimental results (symbols) with the model (curves) described by Eq. (1) for ϕ = 0: ◘, *1* – Mode I; □, *2* – Mode III.

In Figs. 6 to 7 for different phase shifts, the fatigue crack growth rate is expressed versus ΔK parameter for single mode I and for single mode III. From the graphs in Figs. 6 to 7 it appears that, as in Fig. 8, the change of the phase shift from 0 to 90° causes the crack growth rate increase. Moreover (Figs. 6, 7), the value of ΔK parameter is higher for mode I than for mode III for the same fatigue crack growth rate. The Eq. (1) gives satisfactory results for description of the tests. The greater the phase shift was, the fewer values of ΔK were for modes I and III for the same crack growth rate. For example, changing the phase shift from 45° to 90° under the constant crack growth rate $da/dN = 6.0 \cdot 10^{-7}$ m/cycle, we obtain decrease of the stress intensity factor range from ΔK = 68.12 MPa·m$^{1/2}$ to ΔK = 17.32 MPa·m$^{1/2}$ for mode I, and from ΔK = =14.90 MPa·m$^{1/2}$ to ΔK = 3.96 MPa·m$^{1/2}$ for mode III. In Fig. 8 for mixed mode I+III (graphs *1–3*) it can be seen that the change of the phase shift ϕ from 0 to 90° causes an increase of the fatigue crack growth rate.

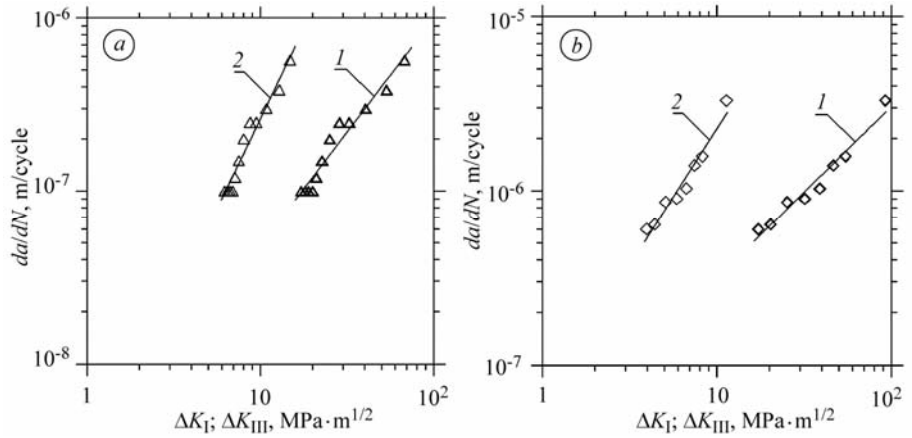

Fig. 7. Comparison of the experimental results (symbols) with the model (curves) described by Eq. (1) for ϕ = 45° (*a*) and for ϕ = 90° (*b*): △,◇, *1* – Mode I; △, ◇, *2* – Mode III.

From the results of the discussed tests for bending with torsion (mixed mode I+III) it appears that are influence of the torsional loading acting with phase shift in relation to bending on the fatigue crack growth rate and specimen life is negative. The least bad influence of torsional loading on the fatigue crack growth in the tested material has been found for proportional loading $\phi = 0$. It results from the high sensitivity of the considered material to torsional loading with phase shift.

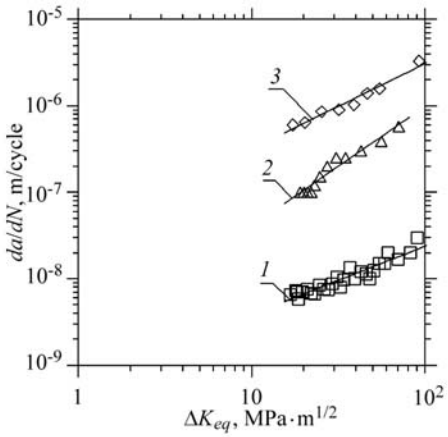

Fig. 8. Comparison of the experimental results (symbols) with the model (curves) described by Eq. (1) for mixed mode I+III. □, *1* – $\phi = 0°$; △, *2* – 45°; ◇, *3* – $\phi = 90°$.

The coefficients *C* and *m* occurring in Eq. (1) were calculated with the least square method and presented in Table 3. It can be seen that for different phase shifts and mixed mode I+III as well as separate modes I and III they take different values. It means that *C* and *m* are not the material constants but they depend on other factors, such as loading. The test results for non-proportional bending with torsion loading include a relative error not exceeding 20% at the significance level $\alpha = 0.05$ for the correlation coefficients *r* given in Table 3. The coefficients of multiple correlation in all the cases take high values, so there is a significant correlation between the experimental results with the assumed Eq. (1).

Table 3. Coefficients *C, m* of Eq. (1) and correlation coefficients *r* for the graphs shown in Figs. 6–8

Figure	C, m(MPa·m$^{1/2}$)$^{-m}$/cycle	m	r
Fig. 6, graph *1*	$1.415 \cdot 10^{-9}$	0.631	0.938
Fig. 6, graph *2*	$7.173 \cdot 10^{-10}$	0.992	0.934
Fig. 7, graph *1*	$2.355 \cdot 10^{-9}$	1.312	0.975
Fig. 7, graph *2*	$2.152 \cdot 10^{-9}$	2.080	0.977
Fig. 8, graph *1*	$3.249 \cdot 10^{-8}$	0.986	0.981
Fig. 8, graph *2*	$6.242 \cdot 10^{-8}$	1.561	0.978
Fig. 9, graph *1*	$6.349 \cdot 10^{-10}$	0.785	0.940
Fig. 9, graph *2*	$1.680 \cdot 10^{-9}$	1.382	0.974
Fig. 9, graph *3*	$3.249 \cdot 10^{-8}$	0.986	0.981

Surfaces of fatigue fractures were analysed (magnification ×13) in order to determine directions of the normal stress (mode I) and the shear stress (mode III). In the cases of mixed modes and phase shifts, principal axes of stresses change their directions. During tests under bending with torsion and proportional loading ($\phi = 0$), the fatigue crack growth proceeded at the angle $\alpha_1 = 37°$, and under the phase shift $\phi = 45°$ – at the angle $\alpha_1 = 19°$, and under $\phi = 90°$ – at $\alpha_1 = 12°$ to the cross section of the specimens. From the tests it appears that as the phase shift angle varies from 0 to 90°, the angle α_1 decreases. It means that phase shift causes transition of the crack growth from the plane of maximum shear stresses to the plane of maximum normal stresses.

CONCLUSIONS

The presented results of the fatigue crack growth in the plane specimens subjected to combined bending with torsional loading allow us to formulate the following conclusions: as the phase shift between bending and torsion decreases from $\phi = 90°$ to

$\phi = 0$, life of the tested material increases; the greater phase shift ϕ is, the fewer values of ΔK are for separate I and III modes under the same crack growth rate; as the phase shift ϕ increases, the inclination angle α_1 between the normal plane of the specimen and the fatigue fracture plane decreases from 37° to 12°.

РЕЗЮМЕ. Подано експериментальні результати втомного росту тріщин в алюмінієвому сплаві AlCu4Mg1 в умовах пропорційного і непропорційного згину з розтягом. Досліджено прямокутні зразки з концентратором на згин. Випроби виконано в умовах високочастотної втоми при $R = -1$ і торсійного навантаження $\phi = 0$; 45° і 90°. Використано лінійне, еліптичне і колове навантаження. Втомний ріст тріщини виміряно за допомогою мікроскопа з 25-кратним збільшенням. Реалізовано I + III моди навантаження. Ріст тріщин на двох бокових поверхнях зразків неоднаковий, проте різниця в довжинах тріщини від концентратора несуттєва. Побудовані діаграми втомного росту тріщини для складного наватаження і показано, що вплив навантаження згином на розмах ΔK у п'ять разів сильніший порівняно з навантаженням закрутом.

РЕЗЮМЕ. Представлены экспериментальные результаты усталостного роста трещин в алюминиевом сплаве AlCu4Mg1 в условиях пропорционального и непропорционального изгиба с растяжением. Использованы прямоугольные образцы с концентратором на изгиб. Исследовали в условиях высокочастотной усталости при $R = -1$ и торсионного нагружения ϕ=0; 45° и 90°. Использовали линейное, эллиптическое и круговое нагружение. Усталостный рост трещины измеряли с помощью микроскопа с 25-кратным увеличением. Реализованы I + III моды нагружения. Рост трещины на двух боковых поверхностях образцов неодинаков, но разница в длине трещины от концентратора несущественна. Построены диаграммы усталостного роста трещины для сложного нагружения и показано, что влияние нагружения изгибом на растяжение ΔK в пять раз сильнее, чем нагружения кручением.

1. *Qian J. and Fatemi A.* Mixed mode fatigue crack growth. A literature survey // Eng. Fracture Mech. – 1996. – **55**. – P. 969–990.
2. *Richard H. A., Fulland M., and Sander M.* Theoretical crack path prediction // Fatigue Fract. Engng. Mater. Struc. – 2005. – **28**. – P. 3–12.
3. *Pook L. P.* The fatigue crack direction and threshold behaviour of mild steel under mixed mode I and III loading // Int. J. Fatigue. – 1985. – **7**. – P. 21–30.
4. *Yates J. R.* Fatigue thresholds under mixed-mode (I+III) loading // Ibid. – 1991. – **13**. – P. 383–388.
5. *Rozumek D. and Macha E.* Elastic-plastic fatigue crack growth in 18G2A steel under proportional bending with torsion loading // Fatigue Fract. Engng. Mater. Struc. – 2006. – **29**. – P. 135–145.
6. *Short* fatigue crack growth under nonproportional multiaxial elastic-plastic strains / R. Döring, J. Hoffmeyer, T. Seeger, and M. Vormwald // Int. J. Fatigue. – 2006. – **28**. – P. 972–982.
7. *Effect* of non-proportional loading paths on the orientation of fatigue crack path / L. Reis, B. Li, M. Leite, and M. Freitas // Fatigue Fract. Engng. Mater. Struc. – 2005. – **28**. – P. 445–454.
8. *Rozumek D.* J-integral in description of fatigue crack growth rate // The Archive of Mechanical Engineering. – 2005. – **LII**. – P. 51–62.
9. *Thum A., Petersen C., and Swenson O.* Verformung, Spannung und Kerbwirkung. – VDI, Duesseldorf, 1960. – P. 73–79.
10. *Rozumek D., Marciniak Z., and Macha E.* Fatigue crack growth rate in non-proportional bending with torsion loading / Eds. J. Pokluda, et al. // Proc. 17th European Conf. of Fracture (ECF17). – Czech Republic: VUTIUM Brno, CD, 2008. – P. 8.
11. *Paris P. C. and Erdogan F.* A critical analysis of crack propagation laws // J. of Basic Eng., Trans. ASME. – 1960. – **85**. – P. 528–534.
12. *Tipton S. M.* Fatigue behaviour under multiaxial loading in the presence of a notch: Methodologies for the prediction of life to crack initiation and life spent in crack propagation. Ph.D. Dissertation, Stanford University, Stanford, California, 1985.
13. *Harris D. O.* Stress intensity factors for hollow circumferentially notched round bars // J. Bas. Engng. – 1967. – **89**. – P. 121–126.
14. *Chell G. G. and Girvan E.* An experimental technique for fast fracture testing in mixed mode // Int. J. Fracture. – 1978. – **14**. – P. 81–84.

Received 22.01.2010